

Nuclear Electric Dipole Moments in Chiral Effective Field Theory

J. Bsaisou^a, J. de Vries^a, C. Hanhart^{a,b}, S. Liebig^a,
Ulf-G. Meißner^{a,b,c,d}, D. Minossi^a, A. Nogga^{a,b}, and A. Wirzba^{a,b}

^a *Institute for Advanced Simulation, Institut für Kernphysik, and Jülich Center for Hadron Physics, Forschungszentrum Jülich, D-52425 Jülich, Germany*

^b *JARA – Forces and Matter Experiments, Forschungszentrum Jülich, D-52425 Jülich, Germany*

^c *JARA – High Performance Computing, Forschungszentrum Jülich, D-52425 Jülich, Germany*

^d *Helmholtz-Institut für Strahlen- und Kernphysik and Bethe Center for Theoretical Physics, Universität Bonn, D-53115 Bonn, Germany*

Abstract

We provide a consistent and complete calculation of the electric dipole moments of the deuteron, helion, and triton in the framework of chiral effective field theory. The CP-conserving and CP-violating interactions are treated on equal footing and we consider CP-violating one-, two-, and three-nucleon operators up to next-to-leading-order in the chiral power counting. In particular, we calculate for the first time EDM contributions induced by the CP-violating three-pion operator. We find that effects of CP-violating nucleon-nucleon contact interactions are larger than those found in previous studies based on phenomenological models for the CP-conserving nucleon-nucleon interactions. Our results which apply to any model of CP violation in the hadronic sector can be used to test various scenarios of CP violation. As examples, we study the implications of our results on the QCD θ -term and the minimal left-right symmetric model.

1 Introduction

Any measurement of a non-vanishing permanent electric dipole moment (EDM) – be it for an electron, nucleon, nucleus, atom or polar molecule with a non-degenerate ground state – would signal the simultaneous violation of parity (P) and time-reversal (T) symmetry and hence the violation of CP symmetry. The complex phase of the Cabibbo-Kobayashi-Maskawa (CKM) matrix of the Standard Model (SM) generates EDMs orders of magnitude smaller [1–4] than the sensitivities of current and planned experiments. Therefore, EDMs serve as ideal probes for *flavor-diagonal* CP violation – with a minimal SM background – from *e.g.* the θ -term of Quantum Chromodynamics (QCD) [5] and *beyond-the-SM* (BSM) physics. Popular examples of the latter are, *e.g.*, supersymmetric, multi-Higgs, or left-right symmetric models. Irrespectively of the high-energy details of such SM extensions, when evolved down to an energy scale where QCD becomes non-perturbative, they give rise to several effective operators of mass dimension six. They are known as the quark EDM (qEDM), quark chromo-EDM (qCEDM), gluon chromo-EDM (gCEDM), and various four-quark interactions [6–8].

Although *one* successful measurement of a non-vanishing EDM would already prove the existence of CP violation beyond the CKM-matrix, it would not be sufficient to reveal the underlying source(s) of CP violation. Independent EDM measurements of single nucleons (neutron and proton) and light nuclei, *e.g.* the deuteron, the helium-3 nucleus (helion) and, maybe, the hydrogen-3 nucleus (triton), and heavier systems such as various atoms and molecules, are in general required to learn more about the underlying source(s). The concept of probing the QCD θ -term and BSM physics using EDMs of light nuclei has attracted much attention in recent years [8–20] and is the basic idea underlying plans for EDM measurements in dedicated storage rings [21–25]. The main advantage of *light* nuclei is that the associated nuclear physics is theoretically well under control, such that these systems can be used to probe the underlying CP-violating mechanism.

The various sources of CP violation at the energy scale $\Lambda_\chi \sim 1$ GeV induce, in principle, an infinite set of CP-violating terms in the effective low-energy pion-nucleon Lagrangian that, however, can be ordered by a power-counting scheme [8, 15, 16, 18, 26]. It was concluded that the leading EDM contributions for nucleons and light nuclei can be expressed in terms of seven interactions:

$$\begin{aligned} \mathcal{L}_{\mathcal{CP}}^{\pi N} = & -d_n N^\dagger (1 - \tau^3) S^\mu v^\nu N F_{\mu\nu} - d_p N^\dagger (1 + \tau^3) S^\mu v^\nu N F_{\mu\nu} \\ & + (m_N \Delta) \pi_3 \pi^2 + g_0 N^\dagger \vec{\pi} \cdot \vec{\tau} N + g_1 N^\dagger \pi_3 N \\ & + C_1 N^\dagger N \mathcal{D}_\mu (N^\dagger S^\mu N) + C_2 N^\dagger \vec{\tau} N \cdot \mathcal{D}_\mu (N^\dagger \vec{\tau} S^\mu N) . \end{aligned} \quad (1.1)$$

Here, $v^\mu = (1, \vec{0})$ and $S^\mu = (0, \vec{\sigma}/2)$ are the nucleon velocity and spin, respectively, $\vec{\tau}$ denotes the vector of the isospin Pauli-matrices τ^i , $\vec{\pi} = (\pi_1, \pi_2, \pi_3)^T$ the pion isospin triplet, \mathcal{D}_μ the covariant derivative acting on the nucleon doublet $N = (p, n)^T$, $m_N = 938.92$ MeV the average nucleon mass [27], and $F_{\mu\nu}$ the electromagnetic field strength tensor. For further notations, we refer to Ref. [28]. The first two interactions in Eq. (1.1) are the neutron (d_n) and proton EDM (d_p), respectively, which are treated as effective parameters here. The second line of Eq. (1.1) contains a purely pionic interaction (with coupling constant Δ) and two pion-nucleon interactions (with coefficients $g_{0,1}$),¹ while the interactions in the last line denote two CP-

¹ Δ , g_0 and g_1 are dimensionless and have the opposite signs of the corresponding dimensionful quantities specified in [8,15]; $\bar{\Delta} = -2F_\pi m_N \Delta$ of Ref. [19] carries dimensions with $F_\pi = 92.2$ MeV the pion decay constant [27].

violating nucleon-nucleon contact terms. Other hadronic interactions, such as the isotensor pion-nucleon interaction $g_2 N^\dagger \pi_3 \tau_3 N$ only appear at orders higher than those considered here.

The different sources of CP violation (*e.g.* the θ -term and dimension-six sources) are expected to contribute to all CP-violating operators in Eq.(1.1), but at different strengths based on the field content and chiral-symmetry properties of the source [10, 15, 16, 18, 19]. Different sources therefore yield different hierarchies of nucleon and nuclear EDM contributions which can explicitly be probed by EDM measurements.

The main goal of this paper is to provide the results of a *complete and consistent* calculation within *chiral effective field theory* (χ EFT)² of the leading single-nucleon, two-nucleon ($2N$) and three-nucleon ($3N$) contributions to the EDMs of light nuclei up-to-and-including next-to-leading order (NLO) with *well defined uncertainties*. The results are expressed as functions of the seven low-energy constants (LECs) in Eq. (1.1), which have to be extracted – in the future – from a combination of EDM measurements and, whenever possible, supplemented with Lattice-QCD calculations.

This paper is organized as follows: the relevant CP-violating operators yielding leading-order (LO) and next-to-leading-order (NLO) EDM contributions for any of the considered sources of CP violation are presented in Section 2, while the employed power-counting scheme is briefly explained in Appendix A. The EDMs of the deuteron, helion and triton as functions of the coefficients in Eq.(1.1) up-to-and-including NLO are computed in Section 3, where χ EFT as well as phenomenological potentials are employed. The main results are presented in Tables 1 and 2 and Eqs.(3.2)–(3.4). As an application of our result, we discuss the cases of the θ -term and minimal left-right symmetric models in Sections 4 and 5, respectively, for which the EDMs of the two- and three-body nuclei can be expressed as functions of a single parameter. We conclude this paper with a brief summary and discussion. Appendix B provides information about the regulator dependence of the EDM contributions resulting from the short-range $4N$ vertices. The small D -wave corrections to the single neutron and proton contributions of the deuteron EDM are missing in the original text. The places where this occurs are marked by a footnote referring to Appendix C which includes an erratum to the published version of the paper.

2 CP-violating nuclear operators

The electric dipole form factor F_3^A for a nucleus $A=^2\text{H}$, ^3He , ^3H is defined by the nuclear matrix element of the *total* CP-violating transition current \tilde{J}^μ . Since CP violation is an extremely small effect, only operators with exactly one insertion of a vertex from Eq. (1.1) need to be considered. The total CP-violating transition current can be written in short-hand notation as

$$\tilde{J}^\mu = J_{\text{CP}}^\mu + V_{\text{CP}} G J^\mu + J^\mu G V_{\text{CP}} + \dots , \quad (2.1)$$

where J^μ (J_{CP}^μ) denotes the CP-conserving (CP-violating) irreducible transition current, V_{CP} the CP-violating potential, and G the complete CP-conserving $2N$ or $3N$ propagator. All operators appearing in Eq. (2.1) are calculated consistently within χ EFT.

The EDM of a nucleus A is most conveniently computed in the Breit-frame, in which the outgoing photon four-momentum equals $q^\mu = (0, \vec{q})$ and \vec{q} can be chosen to point in the z -direction, *i.e.* $\vec{q} = (0, 0, q)$. The CP-violating form factor $F_3^A(q^2)$ and the EDM d_A of a nucleus

²The extension of chiral perturbation theory (ChPT) to systems with more than one nucleon.

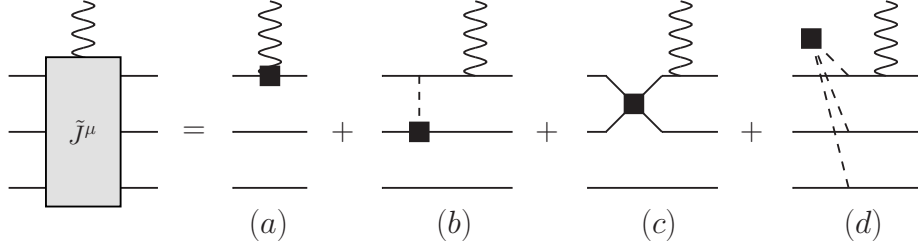


Figure 1: Leading contributions to the total CP-violating $3N$ current. A CP-violating vertex is depicted by a black box. Full, dashed, and wiggly lines refer to nucleons, pions, and photons, respectively. Only one ordering per diagram class is shown. CP-conserving interactions in the intermediate states of diagrams (b)-(d) are not displayed explicitly. When the lowest nucleon line is removed, the diagrams (a)-(c) define the leading contributions for the $2N$ system, too.

A are then given by the following matrix element and its $q^2 \rightarrow 0$ limit, respectively:

$$-iq \frac{F_3^A(q^2)}{2m_A} = \left\langle A; M_J = J \left| \tilde{J}^0(q) \right| A; M_J = J \right\rangle, \quad d_A = \lim_{q^2 \rightarrow 0} \frac{F_3^A(q^2)}{2m_A}. \quad (2.2)$$

Here, J is the total angular momentum of the nucleus of mass m_A and M_J is its z -component.

The nucleons in a $2N$ ($3N$) system can be labelled by an index $i = 1, 2, (3)$. A single-nucleon operator with subindex i is understood to act on nucleon i . The leading single-nucleon contributions to J^μ and the leading single-nucleon contributions induced by the terms in the first line of Eq. (1.1) to $J_{\mathcal{CP}}^\mu$ are ³

$$J_i^\mu = -\frac{e}{2} \left(1 + \tau_{(i)}^3 \right) v^\mu, \quad J_{\mathcal{CP},i}^\mu = -\frac{1}{2} \left[d_n \left(1 - \tau_{(i)}^3 \right) + d_p \left(1 + \tau_{(i)}^3 \right) \right] i\vec{q} \cdot \vec{\sigma}_{(i)} v^\mu. \quad (2.3)$$

Other irreducible CP-conserving and CP-violating current operators only contribute to \tilde{J}^μ at $N^2\text{LO}$ as discussed in [15, 16, 18] and are thus irrelevant for this work.

For $2N$ operators we use the definitions $\vec{\sigma}_{(ij)}^\pm := \vec{\sigma}_{(i)} \pm \vec{\sigma}_{(j)}$, $\tau_{(ij)}^\pm := \tau_{(i)}^\pm \pm \tau_{(j)}^\pm$ with $i \neq j$ and $\vec{k}_i := \vec{p}_i - \vec{p}'_i$, where \vec{p}_i (\vec{p}'_i) is the momentum of an incoming (outgoing) nucleon. The leading $2N$ irreducible potential operators induced by the terms in Eq. (1.1) are [9, 13, 16, 29]

$$\begin{aligned} V_{\mathcal{CP},ij}^{NN}(\vec{k}_i) = & i \frac{g_A}{2F_\pi} \frac{\vec{k}_i}{\vec{k}_i^2 + M_\pi^2} g_0 \vec{\sigma}_{(ij)}^- \vec{\tau}_{(i)} \cdot \vec{\tau}_{(j)} \\ & + i \frac{g_A}{4F_\pi} \frac{\vec{k}_i}{\vec{k}_i^2 + M_\pi^2} \left[g_1 + \Delta f_{g_1}(|\vec{k}_i|) \right] \left(\vec{\sigma}_{(ij)}^+ \tau_{(ij)}^- + \vec{\sigma}_{(ij)}^- \tau_{(ij)}^+ \right) \\ & + \frac{i}{2} \frac{\beta^2 M_\pi^2 \vec{k}_i}{\vec{k}_i^2 + \beta^2 M_\pi^2} \left[C_1 \vec{\sigma}_{(ij)}^- + C_2 \vec{\sigma}_{(ij)}^- \vec{\tau}_{(i)} \cdot \vec{\tau}_{(j)} \right]. \end{aligned} \quad (2.4)$$

Here $g_A = 1.269$ is the axial-vector coupling constant of the nucleon, $F_\pi = (92.2 \pm 0.1)$ MeV the pion decay constant and $M_\pi = 138.01$ MeV the isospin-averaged pion mass [27]. When presenting numerical results, the limit $\beta \rightarrow \infty$ is chosen. The parameter β is introduced only as

³Here and in the following the elementary charge e is defined to be negative, $e < 0$.

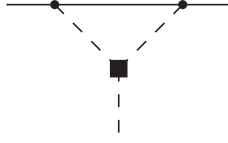


Figure 2: Correction to the g_1 pion-nucleon vertex induced by the CP-violating three-pion vertex in Eq. (1.1). Notation as in Fig. 1.

a diagnostic tool to compare our χ EFT results with those based on phenomenological potentials. The g_1 vertex correction Δf_{g_1} is induced by the three-pion Δ vertex in Eq. (1.1) via the finite one-loop diagram depicted in Fig. 2. This diagram yields [8]

$$f_{g_1}(k) \equiv -\frac{15}{32} \frac{g_A^2 M_\pi m_N}{\pi F_\pi^2} \left[1 + \left(\frac{1 + 2\vec{k}^2/(4M_\pi^2)}{3|\vec{k}|/(2M_\pi)} \arctan \left(\frac{|\vec{k}|}{2M_\pi} \right) - \frac{1}{3} \right) \right], \quad (2.5)$$

where the terms within the brackets have been arranged to indicate the constant and k -dependent components, respectively. The dominant k -independent component of f_{g_1} is larger by a factor of 5π , roughly an order of magnitude, than the power-counting estimate. The enhancement by a numerical factor of π is a common feature of triangular diagrams [26, 30–33], while the factor 5 can be traced back to a coherent sum over isospin.

The three-pion Δ vertex also gives rise to the leading irreducible CP-violating $3N$ potential relevant for the considered $3N$ systems [8, 18],

$$V_{\mathcal{CP}}^{3N}(\vec{k}_1, \vec{k}_2, \vec{k}_3) = -i\Delta \frac{m_N g_A^3}{4F_\pi^3} \left(\delta^{ab} \delta^{c3} + \delta^{ac} \delta^{b3} + \delta^{bc} \delta^{a3} \right) \tau_{(1)}^a \tau_{(2)}^b \tau_{(3)}^c \\ \times \frac{(\vec{\sigma}_{(1)} \cdot \vec{k}_1)(\vec{\sigma}_{(2)} \cdot \vec{k}_2)(\vec{\sigma}_{(3)} \cdot \vec{k}_3)}{\left[\vec{k}_1^2 + M_\pi^2 \right] \left[\vec{k}_2^2 + M_\pi^2 \right] \left[\vec{k}_3^2 + M_\pi^2 \right]}, \quad (2.6)$$

where a, b, c are isospin indices and δ^{ab} is the Kronecker delta. The full CP-violating potential operator $V_{\mathcal{CP}}$ is in general the sum of $V_{\mathcal{CP},ij}^{NN}$, for all permutations of nucleon indices, and $V_{\mathcal{CP}}^{3N}$.

3 The EDMs of the deuteron, the helion and the triton

The CP-conserving wave functions of the deuteron have been computed by solving the scattering equations with the N²LO chiral potential of Refs. [34, 35] for the following five combinations of Lippmann-Schwinger cutoffs Λ_{LS} and Spectral-Function-Regularization cutoffs Λ_{SFR} (see Refs. [34, 35] for a detailed explanation of these cutoffs):

$$(\Lambda_{\text{LS}}, \Lambda_{\text{SFR}}) = \left\{ (0.45, 0.5); (0.6, 0.5); (0.55, 0.6); (0.45, 0.7); (0.6, 0.7) \right\} \text{ GeV}. \quad (3.1)$$

The CP-conserving interactions are here treated non-perturbatively in all orders. Such an approach requires necessarily that cutoffs can only be varied in a limited range. We note that a perturbative treatment of higher orders removes this constraint [36, 37]. The results are, however, equivalent as long as the cutoffs are of the order of 0.5 GeV, which is completely sufficient for this work. With the used range of cutoffs, several LECs of the N²LO chiral potential change sign.

Table 1: Contributions to the deuteron EDM from the N²LO χ EFT potential [34,35], the Av_{18} potential [38] and the CD-Bonn potential [40], respectively. The results from the N²LO χ EFT potential are defined as the center of each interval obtained by employing the five different combinations of LS and SFR cutoffs given in Eq. (3.1). The corresponding *nuclear* uncertainty is the difference between this central value and the boundary values. The results still have to be multiplied by the corresponding coefficients in Eq. (1.1) which here are included in the units. Note that d_n , d_p carry themselves dimensions, namely [e fm], while g_1 and Δ are dimensionless.[§]

label	N ² LO χ EFT	Av_{18}	CD-Bonn	units
d_n	1.00	1.00	1.00	d_n
d_p	1.00	1.00	1.00	d_p
g_1	-0.183 ± 0.017	-0.186	-0.186	$g_1 e$ fm
Δf_{g_1}	0.748 ± 0.138	0.703	0.719	Δe fm

Therefore, we are confident that the employed range of cutoffs is suitable for reliable uncertainty estimates of the CP-violating contributions.

In order to compare our results with previous ones computed from *phenomenological* CP-conserving potentials, the Av_{18} (Av_{18} +UIX) potential [38,39] and the CD-Bonn (CD-Bonn+TM) potential [40,41] have also been applied for the deuteron ($3N$ cases).

The single-nucleon contributions to the deuteron EDM are given by the sum of the neutron and proton EDMs [11] as indicated in the first two rows of Table 1. The deuteron wave function has a 3S_1 and a small 3D_1 component and its isospin is $I=0$. Since the leading contribution to J^μ (see Eq. (2.3)) is spin independent, the convolution of the deuteron wave function with $V_{\mathcal{CP}}$ of Eq. (2.4) has to yield a 3P_1 intermediate state with $I=1$ in order to obtain a nonvanishing complete nuclear matrix element of \tilde{J}^μ [11]. Only the terms proportional to g_1 and Δf_{g_1} in Eq. (2.4) fulfill this isospin selection rule. Their contributions are given in the last two rows of Table 1. The momentum-independent component of $f_{g_1}(\vec{k})$, as defined by the first term in the brackets of Eq. (2.5), amounts to approximately 90% of the total contribution from the Δ -induced g_1 vertex correction.

The listed EDM contributions of the χ EFT potentials are given by the center of the interval resulting from the different cutoff combinations. The pertinent uncertainty is determined from the difference between the center and the boundaries of the interval. We will call this type of uncertainty the *nuclear* uncertainty in order to distinguish it from the *hadronic* uncertainty which is related to the *low-energy* coefficients appearing in Eq. (1.1). The results for the phenomenological potentials considered are also shown in Table 1 and agree (where a comparison is possible) with those in Refs. [9–17]. The values from chiral and phenomenological potentials are in excellent agreement.

The wave functions of the helion and triton have been computed by solving the Faddeev equations for the considered CP-conserving potentials. By a series of arithmetic manipulations [18], the second and third term on the right-hand side of Eq. (2.1) lead to Faddeev equations which

[§]For the D -wave corrected form of the weights of d_n and d_p in Table 1 see Appendix C.

have also been solved numerically. Within this computation both $I = 1/2$ and $I = 3/2$ components of the helion and triton wave functions (with total angular momentum $J = 1/2$) as well as electromagnetic interactions have been considered. The strict isospin selection rule of the deuteron is absent in the helion and triton cases due to a significantly larger number of wave function components and possible intermediate states. All operators in Eq. (2.4) and Eq. (2.6) yield non-vanishing EDM contributions for these nuclei.

Table 2: Contributions to the helion and triton EDMs from the N²LO χ EFT potential with three-nucleon forces [34, 35], the Av_{18} +UIX potential [38, 39] and the CD-Bonn+TM potential [40, 41], respectively. The results are presented as in Table 1. Note that $d_{n,p}$ carry dimension [e fm] and C_i dimension [fm^3].

label	A	N ² LO χ EFT	Av_{18} +UIX	CD-Bonn+TM	units
d_n	³ He	0.904 ± 0.013	0.875	0.902	d_n
	³ H	-0.030 ± 0.007	-0.051	-0.038	d_n
d_p	³ He	-0.029 ± 0.006	-0.050	-0.037	d_p
	³ H	0.918 ± 0.013	0.902	0.876	d_p
Δ	³ He	0.017 ± 0.006	0.015	0.019	Δe fm
	³ H	0.017 ± 0.006	0.015	0.018	Δe fm
g_0	³ He	-0.111 ± 0.013	-0.073	-0.087	$g_0 e$ fm
	³ H	0.108 ± 0.013	0.073	0.085	$g_0 e$ fm
g_1	³ He	-0.142 ± 0.019	-0.142	-0.146	$g_1 e$ fm
	³ H	-0.139 ± 0.019	-0.142	-0.144	$g_1 e$ fm
Δf_{g_1}	³ He	0.608 ± 0.142	0.556	0.586	Δe fm
	³ H	0.598 ± 0.141	0.564	0.576	Δe fm
C_1	³ He	0.042 ± 0.017	0.0014	0.016	$C_1 e$ fm ⁻²
	³ H	-0.041 ± 0.016	-0.0014	-0.016	$C_1 e$ fm ⁻²
C_2	³ He	-0.089 ± 0.022	-0.0042	-0.033	$C_2 e$ fm ⁻²
	³ H	0.087 ± 0.022	0.0044	0.032	$C_2 e$ fm ⁻²

The EDM results are listed in Table 2 for all CP-conserving potentials considered. For the phenomenological potentials, the EDM contributions induced by $d_{n,p}$ and $g_{0,1}$ are in agreement with those of Ref. [17], while the $g_{0,1}$ -induced contributions are smaller than those of Refs. [12, 15] by a factor of two. The dependence of the contributions induced by the C_i vertices on the cutoff parameter β defined in Eq. (2.4) is discussed in Appendix B explicitly for the case of C_2 . The contributions induced by the short-range C_i vertices when the Av_{18} +UIX potential is employed are smaller than the corresponding results reported in Ref. [15]. This discrepancy

might partially be attributed to a deviation similar to the one mentioned before for the $g_{0,1}$ -induced contributions. The slow convergence found in Ref. [15] for χ EFT potentials could not be confirmed within our approach for the N²LO χ EFT potential utilized here. The $d_{n,p}$ and $g_{0,1}$ contributions from the chiral potential and the phenomenological potentials are in reasonable agreement. The largest difference occurs for the g_0 contribution with a 20% – 30% enhancement for the chiral potential.

Next we discuss the contributions from the three-pion Δ vertex which is considered for the first time in this paper. In contrast to the power-counting estimate, the by far dominant contributions arise from the loop-induced g_1 vertex correction. These contributions are larger by roughly a factor of 50 than the contributions from the three-body potential in Eq. (2.6). This discrepancy can only partially be attributed to the enhancement of the one-loop diagram by the factor of 5π mentioned before. Furthermore, the power-counting estimates of the $g_{0,1}$ -induced potential operators modulo $g_{0,1}$ equal the one of the $3N$ CP-violating potential modulo Δ according to Appendix A. The explicit computation of the three-body Δ term yields a contribution that is approximately one order of magnitude smaller than our power-counting scheme predicts. We investigated whether this suppression is related to the high symmetry of the $3N$ wave functions, which are usually dominated by a completely antisymmetric spin-isospin state. However, taking only this principal S -state into account, we found $(0.016 \pm 0.04) \Delta e fm$ for the N²LO χ EFT potential, $0.016 \Delta e fm$ for Av_{18} +UIX potential and $0.018 \Delta e fm$ for CD-Bonn+TM potential, which are very similar to the full results. Therefore, the origin of the discrepancy to the power-counting estimate is not known to us at this point.

The contributions from the short-range C_i vertices, $i = 1, 2$, are highly model-dependent as the last four rows of Table 2 indicate. The Av_{18} (+UIX) and CD-Bonn(+TM) results differ by one order in magnitude and are themselves smaller than the results obtained by employing the N²LO χ EFT potential. The small value of the C_i -contributions for the Av_{18} (+UIX) cases results from an atypically pronounced short-range repulsion of the Av_{18} (+UIX) potential. This can be verified by evaluating the pertinent diagrams with a finite value of β , where β denotes the mass scale in a form factor that is attached to the four-nucleon vertex, *cf.* Eq. (2.4). For $\beta \simeq 3$, which corresponds to cutoffs of the order of 0.5 GeV, the Av_{18} (+UIX) results are in line with the N²LO χ EFT ones. Such cutoffs are standard for implementations of chiral interactions because they lead to natural-sized LECs for four-nucleon vertices. The addition of such a cutoff does not significantly alter the χ EFT results — see also Appendix B.

On the basis of the four, respectively, eight chiral results of Table 1 and Table 2, we find the following predictions for the deuteron, helion and triton EDMs which depend on the low-energy constants of the Lagrangian given in Eq. (1.1):[§]

$$d_{2H} = d_n + d_p - [(0.183 \pm 0.017) g_1 - (0.748 \pm 0.138) \Delta] e fm , \quad (3.2)$$

$$\begin{aligned} d_{3He} = & (0.90 \pm 0.01) d_n - (0.03 \pm 0.01) d_p \\ & + \{ (0.017 \pm 0.006) \Delta - (0.11 \pm 0.01) g_0 - (0.14 \pm 0.02) g_1 + (0.61 \pm 0.14) \Delta \\ & + [(0.04 \pm 0.02) C_1 - (0.09 \pm 0.02) C_2] \times fm^{-3} \} e fm , \end{aligned} \quad (3.3)$$

$$\begin{aligned} d_{3H} = & -(0.03 \pm 0.01) d_n + (0.92 \pm 0.01) d_p \\ & + \{ (0.017 \pm 0.006) \Delta + (0.11 \pm 0.01) g_0 - (0.14 \pm 0.02) g_1 + (0.60 \pm 0.14) \Delta \\ & - [(0.04 \pm 0.02) C_1 - (0.09 \pm 0.02) C_2] \times fm^{-3} \} e fm . \end{aligned} \quad (3.4)$$

[§]For the D -wave corrected form of the d_n and d_p weights in Eq. (3.2) see Appendix C.

The numbers presented here do not in all cases agree with the power-counting estimates in Appendix A. The one-pion-exchange contributions in particular are smaller than the power counting predicts by roughly a factor 3–5, which was also found in Ref. [15]. The main consequence is that the short-range contributions proportional to $C_{1,2}$, which are roughly in agreement with their power-counting estimates, become relatively more important. As discussed above, the three-pion-exchange contributions proportional to Δ are also smaller than expected. We do not know the reason for these discrepancies to the power counting which has been otherwise so successful in many CP-conserving processes. Although the numbers in the Tables 1 and 2 are not always in line with the power-counting estimates, explicit calculations [15, 16, 18] revealed that subleading corrections are indeed suppressed compared with the results listed in Eqs. (3.2)–(3.4). The nuclear uncertainties of the latter terms may be reduced by the replacement of the N²LO CP-conserving chiral potentials and pertinent wave functions by their N³LO counter parts.

The above results for the deuteron, helion, and triton EDMs hold regardless of the underlying mechanism of CP violation. In order to continue the analysis, a particular source (*e.g.* the θ -term, a quark (chromo-)EDM etc.) or a CP-violating high-energy model (in Ref. [19] the minimal left-right symmetric model (mLRSM) and the aligned two-Higgs doublet model were studied) has to be specified. The coefficients of Eq. (1.1) can then be calculated – in the future by Lattice QCD – or estimated within such a particular scenario in order to identify the hierarchies of contributions to the various EDMs, see *e.g.* the analysis in Ref. [42]. In order to focus on the cases of the QCD θ -term and the mLRSM in the two subsequent sections, the discussion in Ref. [19] is briefly repeated and updated.

4 EDMs of light nuclei from the QCD θ -term

4.1 Estimates of the coupling constants in the θ -term scenario

The QCD θ -term can be removed by an axial $U(1)$ transformation at the price of picking up a complex phase of the quark-mass matrix [43]:

$$\mathcal{L}_{\text{QCD}} = \dots + \frac{m_u m_d}{m_u + m_d} \bar{\theta} \bar{q} i \gamma_5 q . \quad (4.1)$$

Since the leading low-energy constants (LECs) of chiral perturbation theory and its heavy-baryon extensions induced by the quark-mass matrix are quantitatively known, the coefficients Δ , g_0 , and g_1 in Eq. (1.1) can be related to quantitatively known matrix elements in the θ -term case [16, 18, 43]. In particular, the three-pion Δ vertex can be related to the strong part of the pion-mass splitting [18, 43],

$$\Delta^\theta = \frac{\epsilon(1 - \epsilon^2)}{16F_\pi m_N} \frac{M_\pi^4}{M_K^2 - M_\pi^2} \bar{\theta} + \dots = (-0.37 \pm 0.09) \cdot 10^{-3} \bar{\theta} , \quad (4.2)$$

with the average kaon mass $M_K = 494.98$ MeV [27] and $\epsilon \equiv (m_u - m_d)/(m_u + m_d) = -0.37 \pm 0.03$ computed from the latest prediction of $m_u/m_d = 0.46 \pm 0.03$ of Ref. [44]. The dots in Eq. (4.2) denote higher-order contributions which are included in the uncertainty estimate. The isospin-breaking pion-nucleon coupling constant g_1 has two leading contributions. The first arises from a shift of the ground state due to the θ -term and is given by

$$g_1^\theta(c_1) = 8c_1 m_N \Delta^\theta = (2.8 \pm 1.1) \cdot 10^{-3} \bar{\theta} , \quad (4.3)$$

which corresponds to $(-7.5 \pm 2.3)\Delta^\theta$ and where $c_1 = (1.0 \pm 0.3) \text{ GeV}^{-1}$ [45] is related to the nucleon sigma term. For details we refer to Refs. [16, 43]. The second contribution, labelled \tilde{g}_1^θ , is currently not quantitatively assessable. It was estimated in Ref. [16] by resonance saturation to equal $\tilde{g}_1^\theta = (0.6 \pm 0.3) \cdot 10^{-3} \cdot \bar{\theta}$, while its Naive Dimensional Analysis (NDA) estimate, cf. Ref. [43], is $|\tilde{g}_1^\theta| \sim |\epsilon| M_\pi^4 / (m_N^3 F_\pi) \sim 1.7 \cdot 10^{-3} \cdot \bar{\theta}$. These estimates can be combined by regarding the result from resonance saturation as the central value and the difference to the NDA estimate as the uncertainty, which yields

$$\tilde{g}_1^\theta = (0.6 \pm 1.1) \cdot 10^{-3} \bar{\theta} . \quad (4.4)$$

This contribution has to be added to $g_1^\theta(c_1)$ to obtain the total value of the g_1^θ coupling constant:

$$g_1^\theta = g_1^\theta(c_1) + \tilde{g}_1^\theta = (3.4 \pm 1.5) \cdot 10^{-3} \bar{\theta} . \quad (4.5)$$

The coefficient of the isospin-conserving CP-violating πN vertex, g_0^θ , is interrelated with the quantitatively known strong contribution to the neutron-proton mass shift, $\delta m_{np}^{\text{str}}$. We do not apply the value for $\delta m_{np}^{\text{str}}$ used in Refs. [16, 18, 19] here, but instead the more refined value $\delta m_{np}^{\text{str}} = (2.44 \pm 0.18) \text{ MeV}$, which follows from a weighted average of the values compiled in Ref. [46] and the newest lattice result of Ref. [47]. We then obtain

$$g_0^\theta = \bar{\theta} \frac{\delta m_{np}^{\text{str}} (1 - \epsilon^2)}{4F_\pi \epsilon} = (-15.5 \pm 1.9) \cdot 10^{-3} \bar{\theta} , \quad (4.6)$$

where the latest update of Ref. [44] for the value of ϵ , see above, has also been included.

The neutron and proton EDMs induced by the θ -term have recently been calculated in Refs. [48, 49] on the basis of supplementary Lattice-QCD input [50–52],

$$d_n^\theta = \bar{\theta} \cdot (2.7 \pm 1.2) \cdot 10^{-16} e \text{ cm} , \quad d_p^\theta = -\bar{\theta} \cdot (2.1 \pm 1.2) \cdot 10^{-16} e \text{ cm} , \quad (4.7)$$

where the signs have been adjusted to our convention $e < 0$.

The coefficients of the nucleon-nucleon contact interactions, $C_{1,2}$, are harder to quantify. In principle they could be deduced from an analysis of isospin-violating pion production in NN collisions studied in Ref. [53] since the CP-violating nucleon-nucleon contact terms are related to the isospin-violating $NN \rightarrow NN\pi$ contact terms in very much the same way as is the g_0 -term to the proton-neutron mass difference.⁴ However, this analysis has not yet been performed with the necessary accuracy. We therefore estimate the strengths of the $C_{1,2}$ via the power-counting estimates of the g_0 -induced two-pion-exchange diagrams since these coefficients should absorb the divergences and associated scale dependences of such diagrams. This procedure yields the estimate

$$|C_{1,2}^\theta| = \mathcal{O} \left(g_0^\theta g_A / (F_\pi m_N^2) \right) \simeq 2 \bar{\theta} \cdot 10^{-3} \text{ fm}^3 , \quad (4.8)$$

while the signs of $C_{1,2}^\theta$ remain unknown. Therefore, the $C_{1,2}$ -induced contributions and their nuclear uncertainties will be added in quadrature to provide an additional – and difficult to reduce – uncertainty to the total EDM results.

⁴This would require a calculation of the isospin-violating $NN \rightarrow NN\pi$ amplitudes to one order higher than currently performed as well as an additional analysis of the reaction $dd \rightarrow \alpha\pi^0$ – the status of the theory for this reaction is reported in Ref. [54] and the latest data is presented in Ref. [55].

4.2 Results for the deuteron and $3N$ EDMs in the θ -term scenario

We can now insert the above predictions for the coefficients in Eq. (1.1) into the power-counting estimates presented in Appendix A. The following hierarchy of nuclear EDM contributions then emerges for the deuteron case: The g_0^θ -induced one-pion exchange and the $C_{1,2}$ -induced contact interactions vanish in the $2N$ system of the deuteron due to isospin selection rules. Therefore, the leading-order EDM contribution is defined by the g_1^θ -induced one-pion exchange [14, 16]. The g_1^θ vertex is corrected by the Δ -dependent term in Eq. (2.4). It generates EDM contributions which are approximately half the size of the tree-level ones induced by the g_1^θ vertex but with the same sign. The only other relevant EDM contribution up to NLO (*i.e.* contributions suppressed by a factor of $\sim M_\pi/m_N$) is the isoscalar sum of the single-nucleon EDMs [15, 16, 56, 57]. In this combination, the large isovector loop contribution to the single-nucleon EDM cancels [58].

Thus the EDM of the deuteron generated by the θ -term up-to-and-including NLO is given by the insertion of d_n^θ , d_p^θ , g_1^θ and Δ^θ into Eq. (3.2):[§]

$$d_{2\text{H}}^\theta = \bar{\theta} \cdot \{ [(0.6 \pm 1.7)] - (0.62 \pm 0.06 \pm 0.28) - (0.28 \pm 0.05 \pm 0.07) \} \cdot 10^{-16} \text{ e cm} . \quad (4.9)$$

In each set of parentheses, the first (second) uncertainty is the nuclear (hadronic) one, except for the sum of single-nucleon contributions, which here only have hadronic uncertainties. Because of the rather large uncertainty of the sum of single-nucleon contributions, the pure two-body contribution[§]

$$d_{2\text{H}}^\theta - d_p^\theta - d_n^\theta = -\bar{\theta} \cdot (0.89 \pm 0.30) \cdot 10^{-16} \text{ e cm} , \quad (4.10)$$

where the uncertainties have been added in quadrature, is more useful to consider. This expression can be applied to extract $\bar{\theta}$ from the measurements of the proton, neutron and deuteron EDMs without additional theoretical input. The contribution of the Δ -induced g_1 vertex correction was not considered in Ref. [19], where therefore a 50% smaller result for the total two-body contribution was obtained.

For the $3N$ systems, the LO EDM contributions – apart from the single-nucleon ones – are defined by the g_0^θ -induced one-pion exchange as depicted in Fig. 1 (b). The g_1^θ -induced one-pion exchange is counted as NLO since $g_1^\theta/g_0^\theta = -0.22 \pm 0.10$. The Δ -dependent correction to g_1 yields contributions which are, as in the deuteron case, roughly one half of the g_1^θ contributions with the same sign. As discussed before, the $3N$ contributions proportional to Δ are smaller than estimated by power counting and are negligible, while the contributions from the CP-violating nucleon-nucleon vertices are accounted for as additional overall uncertainties.

In the order of the rows of Table 2 and the terms in Eqs. (3.3)-(3.4), the different contributions to the helion and triton EDMs induced by the θ -term, respectively, combine to the following

[§]For the D -wave corrected form of the d_n and d_p weights contributing to Eq. (4.9) and appearing in Eq. (4.10) see Appendix C.

total helion and triton EDMs:

$$\begin{aligned}
d_{3\text{He}}^\theta &= \bar{\theta} \cdot \{[(2.44 \pm 0.04 \pm 1.08) + (0.06 \pm 0.01 \pm 0.03)] \\
&\quad - (0.006 \pm 0.002 \pm 0.001) + (1.72 \pm 0.20 \pm 0.21) - (0.48 \pm 0.06 \pm 0.22) \\
&\quad - (0.22 \pm 0.05 \pm 0.05) \pm 0.2\} \cdot 10^{-16} \text{ e cm} \\
&= \bar{\theta} \cdot (3.5 \pm 1.2) \cdot 10^{-16} \text{ e cm} ,
\end{aligned} \tag{4.11}$$

$$\begin{aligned}
d_{3\text{H}}^\theta &= \bar{\theta} \cdot \{[-(0.08 \pm 0.02 \pm 0.04) - (1.93 \pm 0.03 \pm 1.10)] \\
&\quad - (0.006 \pm 0.002 \pm 0.001) - (1.68 \pm 0.20 \pm 0.21) - (0.47 \pm 0.06 \pm 0.21) \\
&\quad - (0.22 \pm 0.05 \pm 0.05) \pm 0.2\} \cdot 10^{-16} \text{ e cm} \\
&= -\bar{\theta} \cdot (4.4 \pm 1.2) \cdot 10^{-16} \text{ e cm} .
\end{aligned} \tag{4.12}$$

In each set of parentheses, the first uncertainty is always the nuclear one, while the second is the hadronic one. In order to remove the influence of the single-nucleon EDM values which rely on Lattice-QCD input at still rather large quark masses, we also list the pure multi-body contributions to the EDMs where the nuclear uncertainty of the single-nucleon terms can safely be neglected:

$$\begin{aligned}
d_{3\text{He}}^\theta - 0.90 d_n^\theta + 0.03 d_p^\theta &= \bar{\theta} \cdot (1.01 \pm 0.42) \cdot 10^{-16} \text{ e cm} , \\
d_{3\text{H}}^\theta - 0.92 d_p^\theta + 0.03 d_n^\theta &= -\bar{\theta} \cdot (2.37 \pm 0.42) \cdot 10^{-16} \text{ e cm} .
\end{aligned} \tag{4.13}$$

Unfortunately, the various nuclear contributions partially cancel for the helion EDM, whereas they add up for the experimentally less interesting triton EDM. This cancellation is the origin of the rather large relative uncertainty of the total helion EDM multi-body contribution. This cancellation was found to be less profound in Ref. [19] since the Δ -dependent correction to g_1^θ was not taken into account. The uncertainties in Eq. (4.13) are dominated by the hadronic uncertainty of the coupling constant g_1^θ , by the nuclear and hadronic uncertainties of the g_0^θ term,⁵ and, finally, by the intrinsic uncertainty due to the CP-violating nucleon-nucleon contact interactions. The latter uncertainty, roughly $\pm 0.2 \cdot 10^{-16} \bar{\theta} \cdot e \cdot \text{cm}$, can be interpreted as the one arising from higher-order corrections and will be difficult to reduce.

5 The minimal left-right symmetric scenario

In this section the implications of our results for the mLRSM scenario are briefly explained. This model and its induced hadronic coupling constants were discussed in detail in the context of hadronic EDMs in Ref. [19] (see also Refs. [59–61]). The predictions of the hadronic coupling constants of Ref. [19] as functions of Δ^{LR} are briefly summarized here before returning the focus on the implications of the results of the nuclear computations presented in this paper.

The mLRSM is based on unbroken parity at high energies by extending the SM gauge symmetry to $SU(2)_R$ [62–69]. Once the additional degrees of freedom – in particular right-handed massive gauge bosons – are integrated out at low energies, the effective Lagrangian contains an additional source of hadronic CP violation in the form of a particular four-quark operator, called

⁵The hadronic uncertainties of g_0^θ and g_1^θ can be reduced by refined predictions of c_1 , $\delta m_{np}^{\text{str}}$ and the quark mass ratio m_u/m_d or difference ϵ , while the nuclear uncertainty might improve by the use of N³LO CP-conserving chiral potentials, see the discussion in Ref. [19].

the four-quark left-right (FQLR) operator [8]. The FQLR operator not only breaks CP symmetry but also chiral and isospin symmetry non-trivially, resulting in a unique pattern of hadronic CP-violating interactions [8, 18]. We assume that there does not appear a θ -term in this model. For discussions of EDMs in left-right models with a nonzero θ -term see, *e.g.*, Refs. [60, 70].

The FQLR operator induces the three-pion vertex in Eq. (1.1) with coupling constant Δ^{LR} as the leading term in the pion sector. According to Refs. [8, 18], the leading contributions to the CP-violating pion-nucleon coupling constants are then the following functions of Δ^{LR} :

$$\begin{aligned} g_1^{LR} &= 8c_1 m_N \Delta^{LR} = (-7.5 \pm 2.3) \Delta^{LR} , \\ g_0^{LR} &= \frac{\delta m_{np}^{\text{str}} m_N \Delta^{LR}}{M_\pi^2} = (0.12 \pm 0.02) \Delta^{LR} . \end{aligned} \quad (5.1)$$

Independent contributions to $g_{1,0}^{LR}$ appear at the same order, which scale as $\tilde{g}_1^{LR} = \mathcal{O}(\Delta^{LR})$ and $\tilde{g}_0^{LR} = \mathcal{O}(\epsilon \Delta^{LR} M_\pi^2 / m_N^2) \simeq 0.01 \Delta^{LR}$ by NDA and are absorbed into the uncertainties of Eq. (5.1) here. The main result is that the ratio $g_0^{LR}/g_1^{LR} \simeq -0.02 \pm 0.01$ is heavily suppressed, such that contributions to hadronic EDMs proportional to g_0^{LR} can be neglected [8].

Moreover, the coefficients $C_{1,2}$ of the isospin-symmetric nucleon-nucleon contact terms are heavily suppressed in the mLRSM due to the need of extra isospin violation. Therefore, these contact terms appear at N⁴LO and can be neglected. There are in principle contributions at N²LO, one order higher than considered in this paper, from the isospin-breaking and CP-violating nucleon-nucleon contact terms

$$\mathcal{L}_{C_{3,4}} = C_3 N^\dagger \tau_3 N \mathcal{D}_\mu (N^\dagger S^\mu N) + C_4 N^\dagger N \mathcal{D}_\mu (N^\dagger \tau_3 S^\mu N) . \quad (5.2)$$

In analogy to the θ -term case, contributions from these contact terms are regarded as the intrinsic uncertainties due to higher-order corrections. Their sizes can be assessed by considering two-pion-exchange diagrams induced by g_1^{LR} to obtain $|C_{3,4}^{LR}| = \mathcal{O}(g_1^{LR} g_A / (F_\pi m_N^2)) \simeq \Delta^{LR} \text{fm}^3$. Their contributions to the deuteron and three-nucleon EDMs read

$$d_{2\text{H}}^{LR}(C_{3,4}^{LR}) \simeq (0.05 \pm 0.05) \cdot (C_4^{LR} - C_3^{LR}) e \text{fm}^{-2} , \quad (5.3)$$

$$d_{3\text{He}}^{LR}(C_{3,4}^{LR}) \simeq d_{3\text{H}}^{LR}(C_{3,4}^{LR}) \simeq [(0.04 \pm 0.03) \cdot C_3^{LR} - (0.07 \pm 0.03) \cdot C_4^{LR}] e \text{fm}^{-2} , \quad (5.4)$$

based on the N²LO χ EFT potential.

The total nuclear contribution to the deuteron EDM induced by the left-right-symmetric scenario is then given by[§]

$$\begin{aligned} d_{2\text{H}}^{LR} - d_p^{LR} - d_n^{LR} &= \Delta^{LR} [(1.37 \pm 0.13 \pm 0.41) + (0.75 \pm 0.14) \pm 0.1] e \text{fm} \\ &= \Delta^{LR} (2.1 \pm 0.5) e \text{fm} , \end{aligned} \quad (5.5)$$

where the first contribution is the one of the g_1^{LR} -induced one-pion exchange, the second – about 55% of the first one – is its three-pion-induced one-loop correction $\Delta^{LR} f_{g_1}$ and the third is the uncertainty from the isospin-violating nucleon-nucleon contact terms. This result for the deuteron EDM allows for an extraction of the parameter Δ^{LR} from EDM measurements of the deuteron, proton and neutron. The nuclear contributions to the helion and triton EDMs provide

[§]For the D -wave corrected form of the d_n and d_p weights in Eq. (5.5) see Appendix C.

a consistency check where again the uncertainties of the single-nucleon contributions can safely be neglected:

$$\begin{aligned}
d_{3\text{He}}^{LR} - 0.90 d_n^{LR} + 0.03 d_p^{LR} &= \Delta^{LR} \{ (0.017 \pm 0.006) - (0.013 \pm 0.002 \pm 0.002) \\
&\quad + (1.07 \pm 0.14 \pm 0.32) + (0.61 \pm 0.14) \pm 0.1 \} e \text{ fm} \\
&= \Delta^{LR} (1.7 \pm 0.5) e \text{ fm} , \tag{5.6}
\end{aligned}$$

$$\begin{aligned}
d_{3\text{H}}^{LR} - 0.92 d_p^{LR} + 0.03 d_n^{LR} &= \Delta^{LR} \{ (0.017 \pm 0.006) + (0.013 \pm 0.002 \pm 0.002) \\
&\quad + (1.04 \pm 0.14 \pm 0.31) + (0.60 \pm 0.14) \pm 0.1 \} e \text{ fm} \\
&= \Delta^{LR} (1.7 \pm 0.5) e \text{ fm} . \tag{5.7}
\end{aligned}$$

The first term in brackets is the Δ^{LR} -induced 3-nucleon contribution, the second and third one stem from the g_0^{LR} - and g_1^{LR} -induced one-pion exchanges, respectively, the fourth corresponds to the $\Delta^{LR} f_{g_1}$ vertex correction, and the fifth is again the uncertainty from the isospin-violating nucleon-nucleon contact terms. As it is the case in Eq. (5.5), the first uncertainty is always the nuclear one and the second, if displayed, is the hadronic one.

The results of Ref. [71] indicate that the single-nucleon EDMs induced by the FQLR operator are significantly smaller than the two- and three-nucleon contributions presented above, although there exists a considerable uncertainty. If the single-nucleon EDM contributions are neglected, there is a non-trivial relation between the considered light-nuclei EDMs induced by the mLRSM [19]:

$$d_{3\text{He}}^{LR} \simeq d_{3\text{H}}^{LR} \simeq 0.8 d_{2\text{H}}^{LR} . \tag{5.8}$$

Note especially that all contributions have the same sign in contradistinction to the θ -term case.

6 Summary and conclusions

In this work we have calculated the EDMs of the deuteron, helion, and triton in the framework of chiral effective field theory. The CP-conserving and -violating nucleon-nucleon potentials and currents are treated on an equal footing and were derived systematically within a controlled power-counting scheme. Up to next-to-leading order in the χ EFT power-counting scheme, nuclear EDMs depend at most on the seven CP-violating hadronic interactions defined in Eq. (1.1), irrespectively of the underlying source of CP violation [8, 15, 16, 18].

We have performed numerical calculations of the EDMs of the three lightest nuclei as functions of these seven coupling constants. Wherever possible, we have compared our results with existing results in the literature [11–13, 15, 17] based on phenomenological CP-conserving potentials and found largely consistent results. While our results for the leading g_0 - and g_1 -induced EDM contributions are in agreement with those of Ref. [17], they are smaller than those of Refs. [12, 15] by a factor of two for the three-nucleon systems. Certain contributions, in particular those dependent on the CP-violating three-pion vertex, have been calculated in this work for the first time. The consistent treatment within χ EFT enabled us to compute the EDMs with well-defined *nuclear* uncertainties which arise from the cutoff dependence of the employed CP-conserving nuclear potential. This uncertainty amounts to approximately 10% for long-range contributions and to almost 50% for short-range contributions. The main results of our work are given in Eqs. (3.2)–(3.4), which summarize the dependence of light-nuclei EDMs on the seven coupling constants. These results are model-independent, *i.e.* they are applicable to any model of CP violation.

In particular, which of the seven interactions dominate(s) the nuclear EDMs does depend on the underlying mechanism of CP violation. However, one can still draw some general conclusions. First of all, contributions from CP-violating nucleon-nucleon contact interactions proved to be less suppressed with respect to one-pion-exchange contributions than chiral power-counting rules indicate. This observation increases the uncertainty of nuclear EDM calculations, but the extent depends on the underlying CP-violating source(s). In addition, this implies that calculations of CP-violating moments of heavier nuclei should not, in general, be performed on the basis of one-pion-exchange potentials only – as is currently state of the art [72] – in order to obtain reliable error estimates. This especially affects analyses of CP-violating models inducing a large gluon chromo-EDM which generates relatively large CP-violating nucleon-nucleon contact terms [15].

Second, we find a significant contribution to nuclear EDMs arising from the one-loop correction of the g_1 vertex of Ref. [15], which is induced by the CP-violating three-pion vertex. The nuclear contributions from this correction turn out to be well approximated by their value at zero-momentum transfer. This means that the three-pion vertex effectively renormalizes the coupling constant g_1 in the case of light nuclei. However, the induced form factor grows linearly with the momentum transfer, which renders momentum-dependent corrections (that cannot be absorbed into g_1) potentially more important for *heavier* systems as the Fermi-scale increases. A detailed calculation for such systems is necessary to quantify this effect.

Third, the three-pion vertex induces a CP-violating three-nucleon potential which power-counting predicts to be significant. However, the full calculations performed here reveal that the three-body potential provides a negligible contribution to the EDMs of the considered three-nucleon systems. Symmetry or other constraints specific to the triton and helion wave functions can be excluded as the reason for this suppression. This CP-violating three-nucleon potential might therefore be safely neglected in nuclear EDM calculations.

Our EDM results can be used to investigate various specific scenarios of CP violation. As two examples, the QCD θ -term and the minimal left-right symmetric scenario were considered here, which can both be traced back to only one dimensionless parameter – of fundamental nature in the former case and of only low-energy effective nature in the latter one. These parameters were discussed in detail in the context of EDMs in Ref. [19]. The θ -term scenario has the advantage that the coupling constants appearing in Eq. (1.1) can be related to known strong matrix elements due to chiral-symmetry considerations. This led to predictions for the nuclear contributions to the deuteron, helion, and triton EDMs as functions of $\bar{\theta}$ directly, see Eqs. (4.10) and (4.13). The uncertainties of the deuteron and triton EDMs are quite small (roughly 30% and 18%, respectively). Unfortunate cancellations among the various nuclear EDM contributions yield a somewhat larger uncertainty (42%) for the experimentally interesting helion EDM.

The uncertainties of our results are governed by the nuclear uncertainty of the isospin-conserving CP-violating one-pion-exchange and nucleon-nucleon contact terms, and especially, by the *hadronic* uncertainties, which arise from the errors of the coupling constants of CP-violating operators. The hadronic uncertainties for the θ -term scenario can be reduced with refined knowledge of the strong part of the neutron-proton mass splitting, $\delta m_{np}^{\text{str}}$, and c_1 which is related to the pion-nucleon sigma term. Their uncertainties are expected to decrease with new Lattice-QCD predictions and a refined analysis of pion-nucleon scattering data (we refer to Ref. [19] for further details). In addition, improved Lattice-QCD calculations of the single-nucleon EDMs would allow for more precise predictions of the total nuclear EDMs. In this case two EDM measurements would be sufficient to confirm the existence of a nonzero θ -term. The nuclear uncertainty of our results can be reduced by the application of N³LO chiral potentials

and associated wave functions.

In the mLRSM scenario it is again possible to use chiral-symmetry considerations to greatly simplify the analysis. All nuclear contributions to the EDMs can be expressed as functions of a single coupling constant, see Eqs. (5.5)–(5.7). Assuming the dominance of the nuclear EDM contributions over the single-nucleon EDM contributions, as expected from chiral perturbation theory [71], the mLRSM predicts the deuteron, helion, and triton EDMs to be of the same sign and (approximately) magnitude. EDM measurements of single nucleons and light nuclei would thus be able to confirm/exclude the mLRSM as the primary origin of the measured EDMs.

More general models can of course be studied in a similar fashion. However, the analysis is then limited by the unknown sizes of the various coupling constants appearing in the model-independent EDM expressions, see Eqs. (3.2)–(3.4). Nevertheless, general statements can still be made using estimates of these coupling constants with unfortunately larger uncertainties (see *e.g.* Refs. [15, 19]). For instance, if the hadronic CP violation is dominated by the quark EDM, the EDMs of light nuclei can be expressed in terms of the single-nucleon EDMs only. On the other hand, in models that induce a large gluon chromo-EDM almost all interactions in Eq. (1.1) contribute to nuclear EDMs at the same order, which makes the analysis extremely complicated. The situation would improve substantially with Lattice-QCD calculations of the coupling constants of CP-violating effective Lagrangian terms induced by the various dimension-six CP-violating operators, see *e.g.* Refs. [73, 74].

In summary, we have performed calculations of light-nuclei EDMs in the framework of chiral effective field theory. We have included CP-violating one-, two-, and three-nucleon interactions up to next-to-leading order in the chiral power counting. We have shown that certain contributions to nuclear EDMs, *e.g.* from nucleon-nucleon contact interactions and the three-pion vertex, which are often neglected in the literature, are actually significant. As applications of our results, we have studied two specific scenarios of CP violation and demonstrated that these could be disentangled with EDM measurements of nucleons and light nuclei. We stress that an important and outstanding challenge in this field is the analog of our Eqs. (3.2)–(3.4) for heavier systems.

Acknowledgements

We are very grateful to Evgeny Epelbaum and Timo Lähde for useful communications. We would also like to thank Stephan Dürr, Emanuele Mereghetti, Tom Luu, Andrea Shindler and Frank Rathmann for discussions. This work is supported in part by the DFG and the NSFC through funds provided to the Sino-German CRC 110 “Symmetries and the Emergence of Structure in QCD”. The resources of the Jülich Supercomputing Center at the Forschungszentrum Jülich, namely the supercomputers JUQUEEN and JUROPA, have been instrumental in the computations reported here.

A Power counting of CP-violating nuclear operators

We estimate the contributions of CP-violating nuclear operators, defined by Eqs. (1.1), (2.3)–(2.6) and (5.2), to the EDMs of light nuclei. The power-counting scheme of Ref. [26] is employed,

Table 3: Power-counting estimates of the leading EDM contributions induced by the coefficients of CP-violating operators defined in Eqs. (1.1), (2.3)–(2.6) and (5.2). The second column displays the estimates for a general source of CP violation, while the third and fourth column show the power-counting estimates for the θ -term and the mLRSM scenario, respectively. Estimates which should be enhanced/suppressed relatively to the power counting are explicitly marked by a star/diamond. The expressions on the right sides of the third and fourth column indicate whether an operator yields a leading-order (LO), a next-to-leading-order (NLO), etc. contribution.

label	general source	θ -term	mLRSM
$d_{n,p}$	$d_{n,p}$	$\bar{\theta} e M_\pi^2/m_N^3$ (NLO)	$\Delta^{LR} e F_\pi/m_N^2$ (N ³ LO)
Δ	$\Delta e F_\pi/M_\pi^2 \diamond$	$\bar{\theta} e F_\pi M_\pi^2/m_N^4 \diamond$ (N ² LO)	$\Delta^{LR} e F_\pi/M_\pi^2 \diamond$ (NLO)
g_0	$g_0 e F_\pi/M_\pi^2$	$\bar{\theta} e F_\pi/m_N^2$ (LO)	$\Delta^{LR} e F_\pi/(M_\pi m_N)$ (N ² LO)
g_1	$g_1 e F_\pi/M_\pi^2$	$\bar{\theta} e F_\pi M_\pi/m_N^3$ (NLO)	$\Delta^{LR} e m_N F_\pi/M_\pi^3$ (LO)
Δf_{g_1}	$\Delta e F_\pi/(M_\pi m_N) *$	$\bar{\theta} e F_\pi M_\pi^3/m_N^5 *$ (N ³ LO)	$\Delta^{LR} e F_\pi/(M_\pi m_N) *$ (N ² LO)
$C_{1,2}$	$C_{1,2} e F_\pi^2$	$\bar{\theta} e F_\pi M_\pi^2/m_N^4$ (N ² LO)	$\Delta^{LR} e F_\pi M_\pi/m_N^3$ (N ⁴ LO)
$C_{3,4}$	$C_{3,4} e F_\pi^2$	$\bar{\theta} e F_\pi M_\pi^3/m_N^5$ (N ³ LO)	$\Delta^{LR} e F_\pi/(M_\pi m_N)$ (N ² LO)

which is also used in Refs. [16, 18]⁶. Within this scheme, the counting orders increase as integer powers of $p/\Lambda_\chi \sim M_\pi/m_N$. To obtain the estimates we take out a common factor from the corresponding diagrams – for the three-body case this normalization factor is $m_N^2/(F_\pi^4 M_\pi^3)$.⁷

While the second column of Table 3 contains the power-counting estimates for a general source of CP-violation with input according to Eqs. (2.3)–(2.6), the third and fourth columns list the estimates for the θ -term and the mLRSM scenarios, respectively. For that purpose, the results of Section 4 for the θ -term case and of Section 5 for the mLRSM scenario have been utilized to assess the numerical sizes of the coefficients, which do not follow in all cases NDA:

- $|g_0^\theta| \sim \bar{\theta} \cdot (M_\pi/m_N)^2$, $|g_1^\theta| \sim (M_\pi/m_N) \cdot |g_0^\theta|$ and $|\Delta^\theta| \sim (M_\pi/m_N)^2 \cdot |g_0^\theta|$ in the θ -term case,
- $|g_1^{LR}| \sim \Delta^{LR} \cdot (M_\pi/m_N)^{-1}$ and $|g_0^{LR}| \sim \Delta^{LR} \cdot (M_\pi/m_N)$ in the mLRSM scenario, and
- $|C_{1,2}| \sim |g_0|/(F_\pi m_N^2)$ and $|C_{3,4}| \sim |g_1|/(F_\pi m_N^2)$ in general.

The second row of Table 3 is specific to a three-body potential and therefore does not apply to the deuteron – on top of the fact that the third and sixth rows are ruled out by isospin selection in this case. The estimates marked by a star (*) in Table 3 should be enhanced by a factor of about 5π relative to the stated order, while the entries marked by a diamond (\diamond) are in reality suppressed by about one order of M_π/m_N – see Section 3 for more details.

⁶The operators relevant for this work are counted in the same way as in the power-counting scheme of Refs. [8, 15]. Differences between these schemes only emerge at one-loop level and in certain currents which have been pointed out in Ref. [16].

⁷One factor of M_π for the photon momentum, *cf.* Eq. (2.2), and one factor of $F_\pi^{-2} \times m_N/M_\pi^2$ per one-pion exchange extracted from the nuclear wave function in such a way that Fig. 1 (a) becomes simply connected.

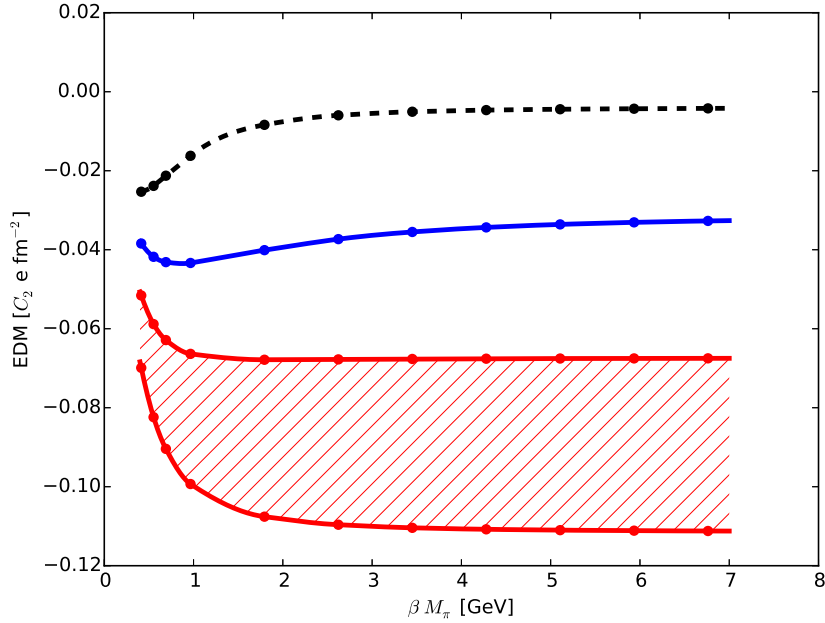


Figure 3: Dependence of the helion EDM contribution induced by the C_2 vertex on the cutoff parameter β . The dashed line depicts the β dependence when the Av_{18} +UIX potential [38, 39] is employed for the CP-conserving component of the nuclear potential, while the solid line shows the β dependence for the CD-Bonn+TM potential [40, 41]. The hatched area depicts the dependence of the C_2 -induced EDM contribution on β and on the cutoffs Λ_{LS} and Λ_{SFR} for the N²LO χ EFT potential [34, 35].

B Regulator dependence of the contact-interaction EDM terms

In order to investigate the EDM contributions from the two-nucleon contact interactions in Eq. (1.1) and Eq. (5.2), an additional cutoff function with parameter β has been introduced — see the third line of Eq. (2.4). As a study case, Figure 3 depicts the β dependence of the contributions to the helion EDM induced by the C_2 vertex when the CP-conserving component of the nuclear potential is given, respectively, by the Av_{18} +UIX potential [38, 39], the CD-Bonn+TM potential [40, 41] or the N²LO χ EFT potential [34, 35] — the latter with the five combinations of cutoffs as in Eq. (3.1).

Modulo a prefactor, the potential operator induced by the C_2 vertex in the third line of Eq. (2.4) coincides with the g_0 -induced potential operator in the first line of Eq. (2.4) for $\beta = 1$. The g_0 -induced contributions to the helion EDM as listed in Table 2 can thus be recovered at $\beta = 1$ by a suitable replacement of units. We have verified explicitly that our numerical calculations are in agreement with this expectation.

The C_i vertices parameterize physics at the momentum scale $\gtrsim 3M_\pi$. For $\beta \leq 3$, the EDM contributions from the Av_{18} +UIX, the CD-Bonn+TM and the N²LO χ EFT potential with the five cutoff combinations are compatible within one order in magnitude since they only differ by a factor of less than three.

To 1% accuracy, the EDM contributions from the N²LO χ EFT potential have converged already if $\beta M_\pi > 3 \text{ GeV}$. The convergence of the corresponding EDM contributions from the $Av_{18}+\text{UIX}$ and the CD-Bonn+TM potentials, however, is more slowly. The discrepancies between the EDM contributions from the three different CP-conserving potentials are especially significant at large βM_π . This reveals the tremendous model dependence in the short-distance regime. The large β limit of $Av_{18}+\text{UIX}$ differs from the one of CD-Bonn+TM by a factor of about eight. As already discussed in Section 3, the small value of the $Av_{18}+\text{UIX}$ limit can be attributed to a large atypical short-range repulsion. The absolute distance between the large β limit of the CD-Bonn+TM case and the β band of the N²LO χ EFT potential is roughly the same as between the β limits of the CD-Bonn+TM and $Av_{18}+\text{UIX}$ cases. The values at $\beta = 49$ were taken as the predictions for the short range EDM contributions given in the last four rows of Table 2 and Eqs. (5.3)-(5.4).

The patterns of convergence with respect to β of the helion EDM contributions induced by the other C_i vertices as well as of their corresponding triton counter parts are similar. Thus they are not explicitly shown here.

C Erratum after publication

As first observed in Ref. [75], the usual weight factors of the neutron (d_n) and proton (d_p) single-nucleon contribution to the electric dipole moment of the deuteron are lacking a small wave-function-dependent term resulting from the subleading 3D_1 component of the deuteron wave function. A simple calculation reveals that the total single-nucleon contribution is

$$d_{2\text{H},\text{single}} = \left(1 - \frac{3}{2} P_D\right) (d_n + d_p),$$

where P_D is the probability of the deuteron 3D_1 -state, which of course depends on the choice of the wave function.

Therefore the values 1.00 of the d_n and d_p weight factors have to be modified in the following places of this paper:

- (i) in the first two rows of Table 1, see the enclosed Table 1',
- (ii) in the first bracket on the right-hand side of Eq. (3.2),

$$d_{2\text{H}} = (0.939 \pm 0.009)(d_n + d_p) - [(0.183 \pm 0.017) g_1 - (0.748 \pm 0.138) \Delta] e \text{ fm}, \quad (3.2')$$

- (iii) implicitly in the first bracket of Eq. (4.9),

$$d_{2\text{H}}^\theta = \bar{\theta} \cdot \{ [(0.56 \pm 0.01 \pm 1.59)] - (0.62 \pm 0.06 \pm 0.28) - (0.28 \pm 0.05 \pm 0.07) \} \cdot 10^{-16} e \text{ cm}, \quad (4.9')$$

such that “(0.6 \pm 1.7)” is replaced by “(0.56 \pm 0.01 \pm 1.59)”, where the first uncertainty is the nuclear one, while the second is the hadronic one,

- (iv) explicitly on the left-hand side of Eq. (4.10),

$$d_{2\text{H}}^\theta - 0.94(d_p^\theta + d_n^\theta) = -\bar{\theta} \cdot (0.89 \pm 0.30) \cdot 10^{-16} e \text{ cm}, \quad (4.10')$$

Table 1': The new entries of Table 1. Captions as in Table 1. Note that the new d_n and d_p weight factors displayed for the Av_{18} potential exactly agree with the ones of Ref. [75].

label	N ² LO χ EFT	Av_{18}	CD-Bonn	units
d_n	0.939 ± 0.009	0.914	0.927	d_n
d_p	0.939 ± 0.009	0.914	0.927	d_p
g_1	-0.183 ± 0.017	-0.186	-0.186	$g_1 \text{ e fm}$
Δf_{g_1}	0.748 ± 0.138	0.703	0.719	$\Delta \text{ e fm}$

(v) and on the left-hand side of Eq. (5.5),

$$\begin{aligned}
 d_{2\text{H}}^{LR} - 0.94(d_p^{LR} + d_n^{LR}) &= \Delta^{LR} [(1.37 \pm 0.13 \pm 0.41) + (0.75 \pm 0.14) \pm 0.1] \text{ e fm} \\
 &= \Delta^{LR} (2.1 \pm 0.5) \text{ e fm} .
 \end{aligned}
 \tag{5.5'}$$

In the latter two cases the uncertainty of the single-nucleon contributions can safely be neglected.

References

- [1] A. Czarnecki and B. Krause, Phys. Rev. Lett. **78**, 4339 (1997), arXiv:hep-ph/9704355.
- [2] M. Pospelov and A. Ritz, Annals Phys. **318**, 119 (2005), arXiv:hep-ph/0504231.
- [3] T. Mannel and N. Uraltsev, Phys. Rev. D **85**, 096002 (2012), arXiv:1202.6270.
- [4] T. Mannel and N. Uraltsev, JHEP **03**, 064 (2013), arXiv:1205.0233.
- [5] G. 't Hooft, Phys. Rev. Lett. **37**, 8 (1976).
- [6] W. Buchmüller and D. Wyler, Phys. Lett. **121B**, 321 (1983).
- [7] B. Grzadkowski, M. Iskrzynski, M. Misiak, and J. Rosiek, JHEP **10**, 085 (2010), arXiv:1008.4884.
- [8] J. de Vries, E. Mereghetti, R. G. E. Timmermans, and U. van Kolck, Annals Phys. **338**, 50 (2013), arXiv:1212.0990.
- [9] I. B. Khriplovich and R. A. Korkin, Nucl. Phys. A **665**, 365 (2000), arXiv:nucl-th/9904081.
- [10] O. Lebedev, K. A. Olive, M. Pospelov, and A. Ritz, Phys. Rev. D **70**, 016003 (2004), arXiv:hep-ph/0402023.
- [11] C.-P. Liu and R. G. E. Timmermans, Phys. Rev. C **70**, 055501 (2004), arXiv:nucl-th/0408060.

- [12] I. Stetcu, C.-P. Liu, J. L. Friar, A. C. Hayes, and P. Navratil, *Phys. Lett. B* **665**, 168 (2008), arXiv:0804.3815.
- [13] I. R. Afnan and B. F. Gibson, *Phys. Rev. C* **82**, 064002 (2010), arXiv:1011.4968.
- [14] J. de Vries, E. Mereghetti, R. G. E. Timmermans, and U. van Kolck, *Phys. Rev. Lett.* **107**, 091804 (2011), arXiv:1102.4068.
- [15] J. de Vries *et al.*, *Phys. Rev. C* **84**, 065501 (2011), arXiv:1109.3604.
- [16] J. Bsaisou *et al.*, *Eur. Phys. J. A* **49**, 31 (2013), arXiv:1209.6306.
- [17] Y.-H. Song, R. Lazauskas, and V. Gudkov, *Phys. Rev. C* **87**, 015501 (2013), arXiv:1211.3762.
- [18] J. Bsaisou, *Electric Dipole Moments of Light Nuclei*, Dissertation, University of Bonn, 2014.
- [19] W. Dekens *et al.*, *JHEP* **07**, 069 (2014), arXiv:1404.6082.
- [20] A. Wirzba, *Nucl. Phys. A* **928**, 116 (2014), arXiv:1404.6131.
- [21] EDM Collaboration, Y. Semertzidis *et al.*, *AIP Conf. Proc.* **698**, 200 (2004), arXiv:hep-ex/0308063.
- [22] Storage Ring EDM Collaboration, Y. K. Semertzidis, (2011), arXiv:1110.3378.
- [23] A. Lehrach, B. Lorentz, W. Morse, N. Nikolaev, and F. Rathmann, (2012), arXiv:1201.5773.
- [24] J. Pretz, *Hyperfine Interact.* **214**, 111 (2013), arXiv:1301.2937.
- [25] JEDI and srEDM Collaborations, F. Rathmann, A. Saleev, and N. N. Nikolaev, *J. Phys. Conf. Ser.* **447**, 012011 (2013).
- [26] S. Liebig, V. Baru, F. Ballout, C. Hanhart, and A. Nogga, *Eur. Phys. J. A* **47**, 69 (2011), arXiv:1003.3826.
- [27] Particle Data Group, K. A. Olive *et al.*, *Chin. Phys. C* **38**, 090001 (2014).
- [28] V. Bernard, N. Kaiser, and U.-G. Meißner, *Int. J. Mod. Phys. E* **4**, 193 (1995), arXiv:hep-ph/9501384.
- [29] C. M. Maekawa, E. Mereghetti, J. de Vries, and U. van Kolck, *Nucl. Phys. A* **872**, 117 (2011), arXiv:1106.6119.
- [30] V. Bernard, N. Kaiser, J. Gasser, and U.-G. Meißner, *Phys. Lett. B* **268**, 291 (1991).
- [31] T. Becher and H. Leutwyler, *Eur. Phys. J. C* **9**, 643 (1999), arXiv:hep-ph/9901384.
- [32] J. L. Friar, U. van Kolck, G. L. Payne, and S. A. Coon, *Phys. Rev. C* **68**, 024003 (2003), arXiv:nucl-th/0303058.
- [33] V. Baru *et al.*, *Eur. Phys. J. A* **48**, 69 (2012), arXiv:1202.0208.

- [34] E. Epelbaum, W. Glöckle, and U.-G. Meißner, Nucl. Phys. A **747**, 362 (2005), arXiv:nucl-th/0405048.
- [35] E. Epelbaum, H.-W. Hammer, and U.-G. Meißner, Rev. Mod. Phys. **81**, 1773 (2009), arXiv:0811.1338.
- [36] M. P. Valderrama, Phys. Rev. C **83**, 024003 (2011).
- [37] M. P. Valderrama, Phys. Rev. C **84**, 064002 (2011).
- [38] R. B. Wiringa, V. G. J. Stoks, and R. Schiavilla, Phys. Rev. C **51**, 38 (1995), arXiv:nucl-th/9408016.
- [39] B. S. Pudliner, V. R. Pandharipande, J. Carlson, S. C. Pieper, and R. B. Wiringa, Phys. Rev. C **56**, 1720 (1997), arXiv:nucl-th/9705009.
- [40] R. Machleidt, Phys. Rev. C **63**, 024001 (2001), arXiv:nucl-th/0006014.
- [41] S. A. Coon and H. K. Han, Few Body Syst. **30**, 131 (2001), arXiv:nucl-th/0101003.
- [42] N. Yamanaka, T. Sato, and T. Kubota, JHEP **12**, 110 (2014), arXiv:1406.3713.
- [43] E. Mereghetti, W. H. Hockings, and U. van Kolck, Annals Phys. **325**, 2363 (2010), arXiv:1002.2391.
- [44] S. Aoki *et al.*, Eur. Phys. J. C **74**, 2890 (2014), arXiv:1310.8555v4.
- [45] V. Baru *et al.*, Nucl. Phys. A **872**, 69 (2011), arXiv:1107.5509.
- [46] A. Walker-Loud, PoS **LATTICE 2013**, 013 (2014), arXiv:1401.8259.
- [47] S. Borsanyi *et al.*, Science **347**, 1452 (2015), arXiv:1406.4088.
- [48] F.-K. Guo and U.-G. Meißner, JHEP **12**, 097 (2012), arXiv:1210.5887.
- [49] T. Akan, F.-K. Guo, and U.-G. Meißner, Phys. Lett. B **736**, 163 (2014), arXiv:1406.2882.
- [50] E. Shintani, S. Aoki, and Y. Kuramashi, Phys. Rev. D **78**, 014503 (2008), arXiv:0803.0797.
- [51] E. Shintani, T. Blum, and T. Izubuchi, PoS **Confinement X**, 330 (2012).
- [52] E. Shintani, Lattice calculation of nucleon EDM, Talk given at “Hadrons from Quarks and Gluons”, Hirschegg, Austria, 2014.
- [53] A. Filin *et al.*, Phys. Lett. B **681**, 423 (2009), arXiv:0907.4671.
- [54] V. Baru, C. Hanhart, and F. Myhrer, Int. J. Mod. Phys. E **23**, 1430004 (2014), arXiv:1310.3505.
- [55] WASA-at-COSY Collaboration, P. Adlarson *et al.*, Phys. Lett. B **739**, 44 (2014), arXiv:1407.2756.
- [56] K. Ottnad, B. Kubis, U.-G. Meißner, and F.-K. Guo, Phys. Lett. B **687**, 42 (2010), arXiv:0911.3981.

- [57] E. Mereghetti, J. de Vries, W. H. Hockings, C. M. Maekawa, and U. van Kolck, Phys. Lett. B **696**, 97 (2011), arXiv:1010.4078.
- [58] R. J. Crewther, P. Di Vecchia, G. Veneziano, and E. Witten, Phys. Lett. **88B**, 123 (1979), [*Erratum ibid.* **91B**, 487 (1980)].
- [59] Y. Zhang, H. An, X. Ji, and R. N. Mohapatra, Nucl. Phys. B **802**, 247 (2008), arXiv:0712.4218.
- [60] A. Maiezza and M. Nemevek, Phys. Rev. D **90**, 095002 (2014), arXiv:1407.3678.
- [61] W. Dekens and D. Boer, Nucl. Phys. B **889**, 727 (2014), arXiv:1409.4052.
- [62] J. C. Pati and A. Salam, Phys. Rev. D **10**, 275 (1974), [*Erratum ibid.* D **11**, 703 (1975)].
- [63] R. N. Mohapatra and J. C. Pati, Phys. Rev. D **11**, 566 (1975).
- [64] R. N. Mohapatra and J. C. Pati, Phys. Rev. D **11**, 2558 (1975).
- [65] G. Senjanovic and R. N. Mohapatra, Phys. Rev. D **12**, 1502 (1975).
- [66] P. Minkowski, Phys. Lett. **67B**, 421 (1977).
- [67] G. Senjanovic, Nucl. Phys. B **153**, 334 (1979).
- [68] R. N. Mohapatra and G. Senjanovic, Phys. Rev. Lett. **44**, 912 (1980).
- [69] R. N. Mohapatra and G. Senjanovic, Phys. Rev. D **23**, 165 (1981).
- [70] R. Kuchimanchi, Phys. Rev. D **91**, 071901 (2015), arXiv:1408.6382.
- [71] C.-Y. Seng, J. de Vries, E. Mereghetti, H. H. Patel, and M. Ramsey-Musolf, Phys. Lett. B **736**, 147 (2014), arXiv:1401.5366.
- [72] J. Engel, M. J. Ramsey-Musolf, and U. van Kolck, Prog. Part. Nucl. Phys. **71**, 21 (2013), arXiv:1303.2371.
- [73] T. Bhattacharya, V. Cirigliano, and R. Gupta, PoS **LATTICE2013**, 299 (2014), arXiv:1403.2445.
- [74] A. Shindler, J. de Vries, and T. Luu, PoS **LATTICE2014**, 251 (2014), arXiv:1409.2735.
- [75] N. Yamanaka and E. Hiyama, (2015), arXiv:1503.04446.